

Articles

New Mechanism for the Intermolecular Hydroamination of Alkynes: Catalysis by Dinuclear Ruthenium Complexes with a Rigid Dicyclopentadienyl Ligand

David P. Klein, Arkady Ellern,[†] and Robert J. Angelici*

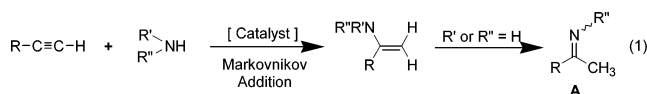
Department of Chemistry, Iowa State University, Ames, Iowa 50011

Received August 11, 2004

The dinuclear ruthenium complex $\{(\eta^5\text{-C}_5\text{H}_3)_2(\text{SiMe}_2)_2\}\text{Ru}_2(\text{CO})_3(\text{C}_2\text{H}_4)\text{H}^+\text{BF}_4^-$ (**1**) catalyzes the intermolecular hydroamination of arylalkynes (e.g., phenylacetylene) with arylamines (e.g., *p*-toluidine) to give imines (e.g., $(\text{Ph}(\text{Me})\text{C}=\text{N}(\text{p-MeC}_6\text{H}_4))$). Although the catalyst has a limited lifetime (up to 6 turnovers), details of the reaction mechanism have been elucidated by isolation and characterization (X-ray and/or NMR) of six of the seven intermediates and reaction-terminating species. The mechanism is fundamentally different from all previously proposed mechanisms for alkyne hydroamination. The rigid doubly bridged bis(dimethylsilyl)cyclopentadienyl ligand is an important feature of the catalyst that facilitates this new type of hydroamination mechanism.

Introduction

Hydroamination of alkynes with amines to give either the corresponding enamine (R' , $\text{R}'' \neq \text{H}$) or imine (R' , $\text{R}'' = \text{H}$) (eq 1) is of great interest because of its potential commercial applications. Hydroamination has been



shown to be catalyzed by a wide variety of early- and late-transition-metal complexes, as well as lanthanide and actinide complexes.¹ Two different mechanisms have been proposed for these reactions: (1) activation of the amine and (2) activation of the alkyne. Amine activation occurs by formation of a metal–imide or metal–amide complex, which reacts further either by a [2 + 2] cycloaddition or by insertion of the alkyne into the metal–nitrogen bond. Alkyne activation occurs by η^2 coordination of the alkyne to the metal through the triple bond, which is subsequently attacked by the amine. Mechanistic studies of this latter route primarily involve the intramolecular hydroamination of alkynes.²

* To whom correspondence should be addressed. E-mail: angelici@iastate.edu.

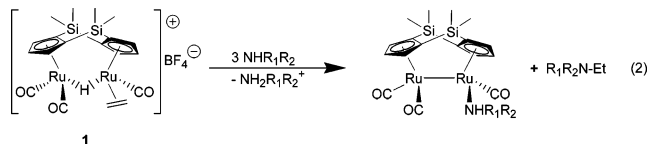
[†] Molecular Structure Laboratory, Iowa State University.

(1) For reviews of alkyne hydroamination see: (a) Alonso, F.; Beletskaya, I. P.; Yus, M. *Chem. Rev.* **2004**, *104*, 3079. (b) Pohlki, F.; Doye, S. *Chem. Soc. Rev.* **2003**, *32*, 104. (c) Müller, T. E. In *Encyclopedia of Catalysis*; Horváth, I. T., Ed.; Wiley-Interscience: New Jersey, 2003; Vol. 3, p 492. (d) Müller, T. E.; Beller, M. *Chem. Rev.* **1998**, *98*, 675.

(2) (a) Müller, T. E.; Berger, M.; Grosche, M.; Herdtweck, E.; Schmidtchen, F. P. *Organometallics* **2001**, *20*, 4384. (b) Müller, T. E.; Grosche, M.; Herdtweck, E.; Pleier, A.-K.; Walter, E.; Yan, Y.-K. *Organometallics* **2000**, *19*, 170. (c) Müller, T. E.; Pleier, A.-K. *J. Chem. Soc., Dalton Trans.* **1999**, 583.

There are few reports³ of hydroaminations involving catalytic species that contain more than one metal center; however, the hydroamination of arylalkynes by arylamines is catalyzed by ruthenium carbonyl, $\text{Ru}_3(\text{CO})_{12}$.³ For this reaction, the authors proposed an amine activation mechanism but could not exclude alkyne coordination as a possible first step in the catalytic cycle.^{3a}

Recently, our group reported the stoichiometric hydroamination of alkenes in the reaction (eq 2) of amines with $\{(\eta^5\text{-C}_5\text{H}_3)_2(\text{SiMe}_2)_2\}\text{Ru}_2(\text{CO})_3(\text{C}_2\text{H}_4)\text{H}^+\text{BF}_4^-$ (**1**), which contains the doubly linked bis(dimethylsilyl)cyclopentadienyl ligand.⁴ Addition of 3 equiv of amine



yields the alkylated amine as a result of a Markovnikov addition of the amine to the coordinated olefin. Attempts to make this system catalytic were unsuccessful, presumably because the alkylated ammonium ion ($^+\text{NH}_2\text{-R}_1\text{R}_2$) is unable to reprotonate the Ru–Ru bond.⁵ The hydroamination of alkynes generally occurs more readily¹ than that of alkenes; therefore, we explored the use of **1** as a catalyst for alkyne hydroamination. Herein, we report the results of these catalytic experiments, with

(3) (a) Uchimaru, Y. *Chem. Commun.* **1999**, 1133. (b) Tokunaga, M.; Eckert, M.; Wakatsuki, Y. *Angew. Chem., Int. Ed.* **1999**, *38*, 3222. (c) Kondo, T.; Okada, T.; Suzuki, T.; Mitsudo, T. *J. Organomet. Chem.* **2001**, *622*, 149.

(4) Ovchinnikov, M. V.; LeBlanc, E.; Guzei, I. A.; Angelici, R. J. *J. Am. Chem. Soc.* **2001**, *123*, 11494.

(5) Klein, D. P.; Angelici, R. J. Unpublished results.

Table 1. Hydroamination of Acetylenes Catalyzed by 1, 2, 3a,b, and 8

entry ^a	acetylene	amine	solvent	TO ^b (% yield)
1	PhC≡CH	<i>p</i> -MeC ₆ H ₄ NH ₂	CD ₂ Cl ₂	3.3 (11)
2 ^c	PhC≡CH	<i>p</i> -MeC ₆ H ₄ NH ₂	CD ₂ Cl ₂	NR
3 ^{d,e}	PhC≡CH	<i>p</i> -MeC ₆ H ₄ NH ₂	CD ₂ Cl ₂	3.5 (12)
4 ^f	PhC≡CH	<i>p</i> -MeC ₆ H ₄ NH ₂	CD ₂ Cl ₂	5.0 (17)
5 ^e	PhC≡CH	<i>p</i> -MeC ₆ H ₄ NH ₂	CD ₂ Cl ₂	NR
6 ^g	PhC≡CH	<i>p</i> -MeC ₆ H ₄ NH ₂	CD ₂ Cl ₂	NR
7 ^h	PhC≡CH	<i>p</i> -MeC ₆ H ₄ NH ₂	CD ₂ Cl ₂	4.1 (14)
8 ⁱ	PhC≡CH	<i>p</i> -MeC ₆ H ₄ NH ₂	CD ₂ Cl ₂	2.9 (29)
9 ^j	PhC≡CH	<i>p</i> -MeC ₆ H ₄ NH ₂	CD ₂ Cl ₂	3.5 (12)
10	<i>n</i> -hexC≡CH	<i>p</i> -MeC ₆ H ₄ NH ₂	CD ₂ Cl ₂	1.8 (6.2)
11	Me ₃ SiC≡CH	<i>p</i> -MeC ₆ H ₄ NH ₂	CD ₂ Cl ₂	NR
12	<i>o</i> -MeC ₆ H ₄ C≡CH	<i>p</i> -MeC ₆ H ₄ NH ₂	CD ₂ Cl ₂	NR
13	<i>p</i> -FC ₆ H ₄ C≡CH	<i>p</i> -MeC ₆ H ₄ NH ₂	CD ₂ Cl ₂	5.8 (20)
14	<i>p</i> -CF ₃ C ₆ H ₄ C≡CH	<i>p</i> -MeC ₆ H ₄ NH ₂	CD ₂ Cl ₂	NR
15	PhC≡CMe	<i>p</i> -MeC ₆ H ₄ NH ₂	CD ₂ Cl ₂	NR
16	PhC≡CPh	<i>p</i> -MeC ₆ H ₄ NH ₂	CD ₂ Cl ₂	NR
17 ^{i,k}	PhC≡CH	<i>p</i> -MeC ₆ H ₄ NH ₂	(CD ₃) ₂ SO	NR
18	PhC≡CH	<i>p</i> -MeC ₆ H ₄ NH ₂	(CD ₃) ₂ CO	NR
19 ^{i,l}	PhC≡CH	<i>p</i> -MeC ₆ H ₄ NH ₂	(CD ₃) ₂ CO	NR
20	PhC≡CH	<i>n</i> -PrNH ₂	CD ₂ Cl ₂	NR
21	PhC≡CH	PhNHMe	CD ₂ Cl ₂	NR
22 ^{d,e}	PhC≡CH	PhNH ₂	CD ₂ Cl ₂	3.6 (12)
23 ^m	PhC≡CH	<i>p</i> -MeC ₆ H ₄ NH ₂	CD ₂ Cl ₂	0.82 (2.8)

^a Conditions (unless otherwise indicated): all reaction mixtures contain 0.35 mmol of acetylene, 0.35 mmol of amine, 0.012 mmol (3.3 mol %) of **1**, and 0.6 mL of CD₂Cl₂; 40 ± 1.0 °C, 18 h. ^b Turnovers (TO) are determined from NMR product integrations vs *N,N*-dimethylacetamide as internal standard; percent yields are based on NMR yields relative to the indicated acetylene and are the average of two runs (±10%). ^c 25.0 ± 0.1 °C. ^d 0.012 mmol of HBF₄·OEt₂ added. ^e **2** catalyst. ^f 0.35 mmol of acetylene, 0.35 mmol of *p*-toluidine, 0.056 mmol of (*p*-MeC₆H₄)NH₃⁺BF₄⁻, and 0.012 mmol (3.3 mol %) of **2** added. ^g 0.35 mmol of acetylene, 0.47 mmol of amine and 0.12 mmol of HBF₄·OEt₂ added. ^h **8** catalyst. ⁱ 0.035 mmol of (10 mol %) **1**. ^j 1.05 mmol of amine. ^k 18 h at 50 ± 1 °C. ^l 18 h at 65 ± 1 °C. ^m {(η⁵-C₅H₅)₂Ru₂(CO)₂(μ-CO){μ₂-η¹:η²-C(Ph)-CH₂}⁺BF₄⁻ catalyst.

special attention directed at understanding the mechanism of this catalytic hydroamination reaction. The mechanistic study was accomplished by independent syntheses and characterizations of some of the proposed intermediates in the catalytic cycle and by studies of the inactivation of the catalyst. Of particular note is the importance of the doubly linked bis((dimethylsilyl)cyclopentadienyl) ligand and the Ru–Ru unit in promoting the catalysis by **1**.

Results and Discussion

Intermolecular Hydroamination Catalyzed by Complexes 1, 2, 3a,b, and 8. Catalytic reactions (eq 1) of alkynes with amines to give an imine (**A**) are summarized in Table 1. Typically, 0.35 mmol of an alkyne is reacted with 0.35 mmol of an amine in the presence of 0.012 mmol of a catalyst precursor (**1**, **2**, **3a,b**, or **8**) for 18 h at 40 °C; longer reaction times did not give yields any higher than those reported in Table 1. These reactions gave no evidence for other products, and there was also no evidence of anti-Markovnikov addition. Unreacted alkyne, amine, and vinylidene complex **6** (see below) were the only other species present at the end of the reaction. The reaction of phenylacetylene with *p*-toluidine (eq 1) at 40 °C is catalyzed by complex **1** to give *N*-(*p*-tolyl)phenylmethanimine in 11% yield, corresponding to 3.3 turnovers (entry 1); this reaction does not occur at a significant

rate at 25 °C (entry 2). Increasing the catalyst (**1**) concentration by a factor of 3 increased the yield to 29%, but the number of turnovers remained at 2.9 (entry 8). A 3-fold increase in the amine concentration does not change the yield of the reaction (3.5 turnovers, 12% yield, entry 9).

The reaction of phenylacetylene with *p*-toluidine is also catalyzed by {(η⁵-C₅H₅)₂(SiMe₂)₂}Ru₂(CO)₂(μ-CO){μ₂-η¹:η¹-C(Ph)=C(H)} (**2**; see Scheme 1) in the presence of equimolar HBF₄·OEt₂, which immediately protonates the amine to give 1 equiv of RNH₃⁺BF₄⁻; this reaction gives a slightly higher yield (entry 3, 12% yield, 3.5 turnovers) than with **1** as the catalyst (entry 1). When approximately 4.5 equiv of RNH₃⁺BF₄⁻ is added (entry 4), the number of turnovers increases to 5.0 (17% yield). The hydroamination reaction is not catalyzed by **2** in the absence of acid (entry 5), and catalyst **2** is essential to the reaction, as no hydroamination occurs when phenylacetylene is combined with *p*-toluidine and HBF₄·OEt₂ under the standard reaction conditions (entry 6). The *p*-toluidine complex {(η⁵-C₅H₅)₂(SiMe₂)₂}Ru₂(CO)₃{NH₂(*p*-MeC₆H₄)}H⁺BF₄⁻ (**8**) also catalyzes the reaction of *p*-toluidine and phenylacetylene (entry 7) to give the imine product in 14% yield (4.1 turnovers).

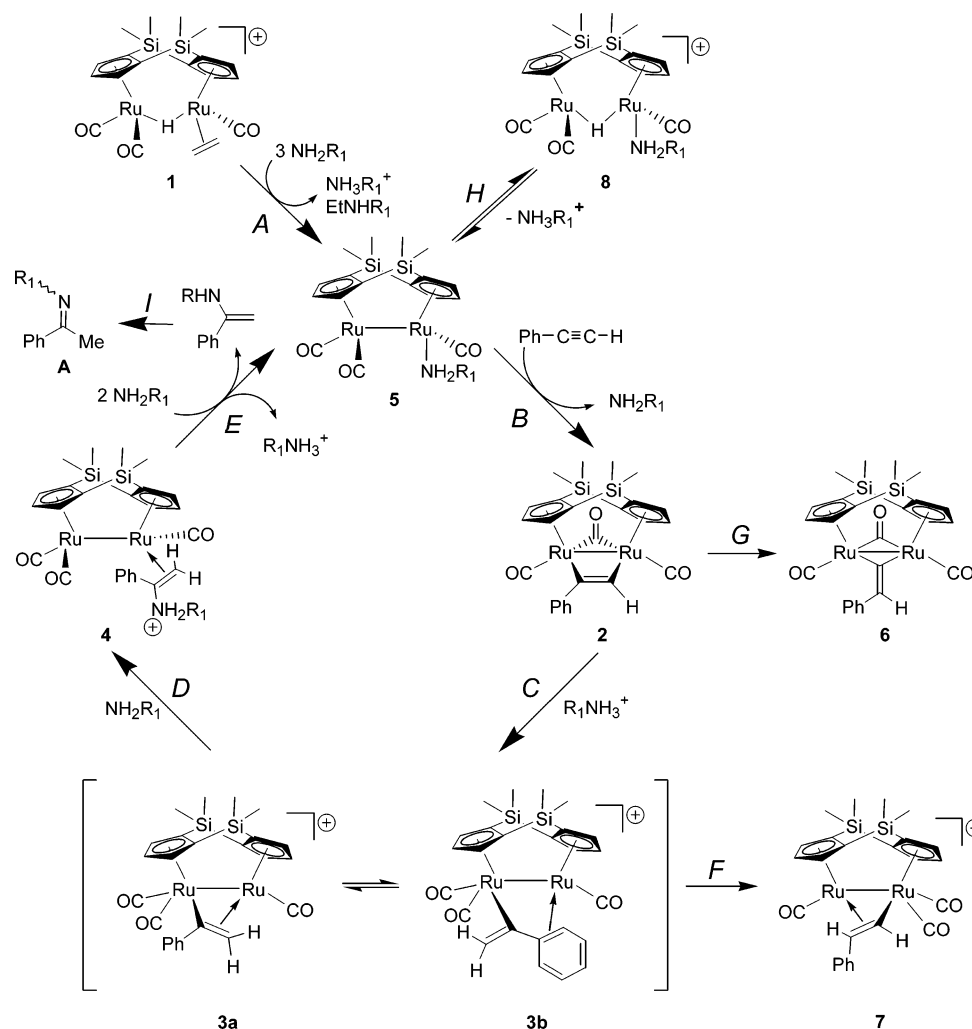
As observed in studies of other hydroamination reactions,³ aliphatic alkynes are not as reactive as arylalkynes; this is evident in the reaction of 1-octyne with *p*-toluidine (entry 10), which gives only a 6.2% yield (1.8 turnovers) of *N*-(2-octylidene)-4-methylaniline, as compared with a 11% yield for the same reaction with phenylacetylene. Under the same conditions, (trimethylsilyl)acetylene does not react (entry 11), presumably because of the bulky nature of the SiMe₃ group. Phenylacetylene with an *o*-methyl group is also unreactive (entry 12), again presumably due to a steric effect. Reduction of the electron density in the phenyl ring by incorporation of an electron-withdrawing *p*-fluoro group increases the yield of the reaction to 20% (5.8 turnovers, entry 13). However, the more strongly electron-withdrawing *p*-trifluoromethyl group results in no reaction (entry 14). Internal alkynes (entries 15 and 16) do not react with *p*-toluidine in the presence of catalyst. In an attempt to increase the overall rate of reaction by increasing the temperature, the higher boiling solvents (CD₃)₂SO and (CD₃)₂CO (entries 17–19) were used, but they inactivated the catalyst, most likely by coordination to the metal center.

From studies of the reactions of phenylacetylene with different amines, it is evident that the p*K*_a and steric properties of the amines affect their reactions. Amines with a higher p*K*_a (*n*-propylamine, p*K*_a(H₂O) = 10.8,⁶ entry 20) or larger cone angle (*N*-methylaniline, cone angle 126°,⁷ entry 21) than *p*-toluidine (p*K*_a(H₂O) = 5.1,⁶ cone angle 111°)⁷ do not react; however, a decrease in amine p*K*_a(H₂O) to 4.6 by the use of aniline⁶ (entry 22) results in the same yield of the product imine (3.6 turnovers, 12% yield). The reaction is not catalyzed by the nonbridged cyclopentadienyl complex {(η⁵-C₅H₅)₂-Ru₂(CO)₂(μ-CO){μ₂-η¹:η²-C(Ph)=CH₂}⁺BF₄⁻ (0.82 turnovers, entry 23), which indicates the importance of the bridging (η⁵-C₅H₅)₂(SiMe₂)₂ ligand. In {(η⁵-C₅H₅)₂Ru₂-

(6) Perrin, D. D. *Dissociation Constants of Organic Bases in Aqueous Solution*; Butterworth: London, 1972.

(7) Seligson, A. L.; Troglor, W. C. *J. Am. Chem. Soc.* **1991**, *113*, 2520.

Scheme 1



(CO)₂(μ-CO){μ₂-η¹:η²-C(Ph)=CH₂}⁺BF₄⁻, the -C(Ph)=CH₂ group is the same as that in **3a**, but the cyclopentadienyl ligands are oriented trans to each other,⁸ which may be a reason for the inactivity of the nonbridged complex in hydroamination catalysis.

Considering the above data, the best catalytic performance is achieved in a system that utilizes a primary arylamine, a phenylacetylene with a moderately electron-withdrawing group, the weakly coordinating solvent methylene chloride, and the preformed catalyst precursor **2** in the presence of excess HBF₄·OEt₂. Although there are other more efficient routes for the synthesis of the arylimines produced in these reactions, the low reactivity and relatively short lifetimes of the catalyst have allowed us to understand the mechanism of the catalytic reactions and events that lead to inactivation of the catalyst, as described in the next section.

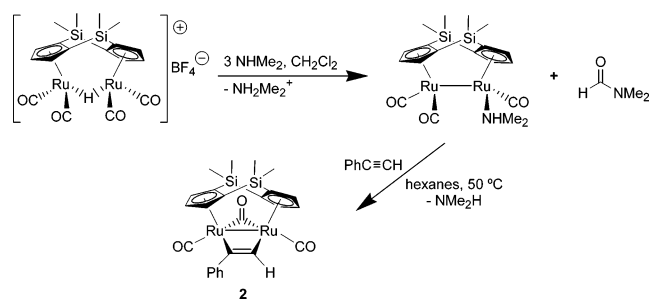
Proposed Mechanism for the Hydroamination of Alkynes as Catalyzed by Complexes 1, 2, 3a, b, and 8. On the basis of results of the catalytic reactions described above, as well as experiments described below, a mechanism for the hydroamination of phenylacetylene is proposed in Scheme 1. In this mechanism, when complex **1** is the catalyst precursor, the first step is the

removal of the ethylene and H⁺ ligands by the known nucleophilic amine attack (eq 2) to give NH(*p*-MeC₆H₄)-Et and amine complex **5** (step A).⁴ In step B, phenylacetylene displaces the amine to give complex **2**, which then undergoes protonation by the *p*-toluidinium ion to give an equilibrium mixture of complexes **3a, b** (step C). One or both of these cationic complexes is activated to attack by *p*-toluidine (step D) to give the cationic complex **4**. In step E, the enaminium ligand is displaced directly by *p*-toluidine or the amine first deprotonates the enaminium ligand followed by displacement of the enamine by another molecule of amine to give {(η⁵-C₅H₃)₂(SiMe₂)₂}Ru₂(CO)₃(NH₂(*p*-MeC₆H₄)) (**5**), which is in equilibrium with the protonated complex **8**. The observed imine product (**A**) is formed by a 1,3-hydrogen shift in the enamine (step J). The catalytic reaction ends, due to the conversion of **2** to the bridging vinylidene complex (**6**), which is catalytically inactive and is the only Ru-containing product observed at the end of the reaction (step G). In the following paragraphs we describe the evidence for each of the steps in the proposed mechanism.

The only Ru-containing species observed in ¹H NMR spectra of CD₂Cl₂ solutions of the catalytic reactions of phenylacetylene, *p*-toluidine, and **1** is complex **2**, which is the resting state of the catalyst. This complex has been independently synthesized (Scheme 2) by the

(8) Dyke, A. F.; Knox, S. A. R.; Morris, M. J.; Naish, P. J. *J. Chem. Soc., Dalton Trans.* **1983**, 1417.

Scheme 2



reaction of $\{(\eta^5\text{-C}_5\text{H}_3)_2(\text{SiMe}_2)_2\}\text{Ru}_2(\text{CO})_4\text{H}^+\text{BF}_4^-$ with NMe_2H to give $\{(\eta^5\text{-C}_5\text{H}_3)_2(\text{SiMe}_2)_2\}\text{Ru}_2(\text{CO})_3(\text{NHMe}_2)$, which is subsequently reacted with phenylacetylene at 50 °C to give **2**. This synthesis makes use of the known reaction of $\{(\eta^5\text{-C}_5\text{H}_3)_2(\text{SiMe}_2)_2\}\text{Ru}_2(\text{CO})_4\text{H}^+\text{BF}_4^-$ with amines to give amine complexes.⁹ Formation of **2** occurs by displacement of the NHMe_2 ligand from the amine complex. Complex **2** contains an $\mu_2\text{-}\eta^1\text{:}\eta^1$ -phenylacetylene ligand that bridges both Ru atoms through both C atoms of the carbon–carbon triple bond. The unsymmetrical nature of complex **2** is evident in the ^1H NMR spectrum, which shows two inequivalent Cp fragments; each fragment shows a triplet and two doublets, with resonances for the Cp hydrogen atoms at δ 5.21 (m), 5.26 (m), 5.66 (m), 5.69 (m), 6.41 (t), and 6.43 (t). The lack of symmetry in the $(\eta^5\text{-C}_5\text{H}_3)_2(\text{SiMe}_2)_2$ ligand is also reflected in the four different resonances for the four Si–Me groups with signals at 0.27, 0.37, 0.45, and 0.52 ppm. The resonance for the acetylenic proton is observed as a singlet at 8.46 ppm, which is 0.85 ppm downfield from that observed in the bridging vinylidene isomer (**6**, Scheme 1).¹⁰ The ^{13}C NMR spectrum, which is consistent with the structure of **2**, exhibits 4 signals for the Si–Me groups, 10 resonances for the Cp fragments, 3 signals for the CO ligands, and 1 broad resonance at 104.13 ppm for the acetylenic carbons. The infrared spectrum of **2** in the $\nu(\text{CO})$ region shows absorptions at 1996 (vs), 1965 (s), and 1772 (w) cm^{-1} , the last signal for a bridging CO group.

The molecular structure of **2** has been determined by X-ray diffraction (Figure 1) and exhibits a Ru–Ru bond that is bridged by both the phenylacetylene unit and a carbon monoxide. The Ru(1)–Ru(2) bond length of 2.7661 Å is elongated (0.11 Å) compared to that in the bridging vinylidene isomer **6** (2.6551 Å).¹⁰ The Cp–Cp fold angle (122.68°) in **2** is 4° larger than that in the bridging vinylidene complex, which is consistent with the longer Ru–Ru bond distance. The Ru–Cp(centroid) distances (average 1.91 Å) are nearly identical with those in the bridging vinylidene complex (**6**, average 1.92 Å), and there is virtually no twist between the two Cp fragments ($\angle\text{Cp}(\text{centroid})\text{-Ru}(1)\text{-Ru}(2)\text{-Cp}(\text{centroid}) = 1.2^\circ$). The terminal CO ligands lie nearly in the same plane shared by the two Ru atoms and the Cp centroids. Interestingly, the carbon–carbon distances of the bridging phenylacetylene (C(17)–C(18)) in **2** and **6** are identical at 1.31 Å,¹⁰ a distance that is between that of a carbon–carbon double (1.34 Å) and triple bond

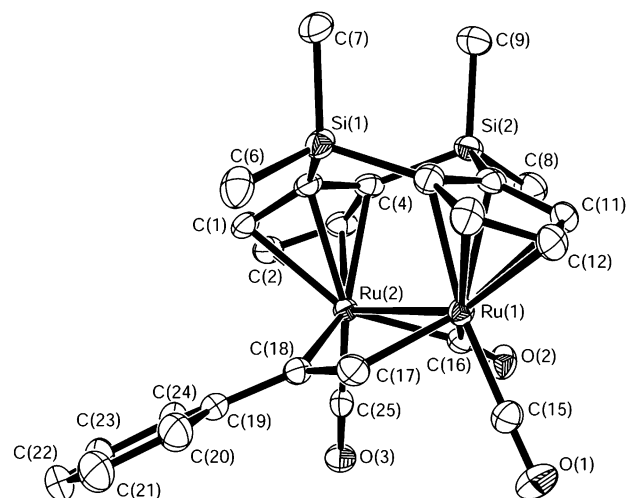


Figure 1. Thermal ellipsoid drawing of $\{(\eta^5\text{-C}_5\text{H}_3)_2(\text{SiMe}_2)_2\}\text{Ru}(\text{CO})_2(\mu\text{-CO})\{\mu_2\text{-}\eta^1\text{:}\eta^1\text{-C}(\text{Ph})=\text{C}(\text{H})\}$ (**2**) with 50% ellipsoid probability and labeling scheme. Hydrogen atoms are omitted for clarity. Selected bond distances (Å) and angles (deg): Ru(1)–Ru(2), 2.7661(4); Ru(1)–C(17), 2.082(3); Ru(2)–C(18), 2.103(3); C(17)–C(18), 1.311(4); C(18)–C(19), 1.486(4); Ru(1)–Cp(centroid), 1.913; Ru(2)–Cp(centroid), 1.920; $\angle\text{C}(15)\text{-Ru}(1)\text{-C}(16)$, 82.7(1); $\angle\text{C}(15)\text{-Ru}(1)\text{-C}(17)$, 83.6(1); $\angle\text{C}(16)\text{-Ru}(1)\text{-C}(17)$, 101.8(1); $\angle\text{Ru}(1)\text{-C}(17)\text{-C}(18)$, 113.8(2); $\angle\text{Ru}(2)\text{-C}(18)\text{-C}(17)$, 106.9(2); $\angle\text{C}(17)\text{-C}(18)\text{-C}(19)$, 127.6(3); $\angle\text{Ru}(2)\text{-C}(18)\text{-C}(19)$, 125.4(2); $\angle\text{Ru}(1)\text{-C}(16)\text{-Ru}(2)$, 85.6(1); $\angle\text{C}(15)\text{-Ru}(1)\text{-Ru}(2)\text{-C}(25)$, 4.6; $\angle\text{C}(20)\text{-C}(19)\text{-C}(18)\text{-C}(17)$, 13; $\angle\text{Ru}(2)\text{-C}(18)\text{-C}(17)\text{-Ru}(1)$, 2.3; $\angle\text{Cp}(\text{centroid})\text{-Ru}(1)\text{-Ru}(2)\text{-Cp}(\text{centroid})$, 1.2; $\angle\text{Cp}\text{-Cp}$ fold angle, 122.68.

(1.20 Å). This bond is only 2.24° out of parallel with the Ru–Ru bond. The C(17), C(18), and C(19) atoms of the phenylacetylene ligand and the two Ru centers lie in the same plane, as evidenced by the torsion angles Ph(centroid)–C(18)–C(17)–Ru(1) (1°) and Ru(2)–C(18)–C(17)–Ru(1) (2°).

The resting state of the catalyst during the reaction is complex **2**, as it is observed during the course of the reaction by the presence of Si–Me resonances at 0.27, 0.37, 0.45, and 0.52 ppm in the ^1H NMR spectrum in as little as 1 h after the start of the reaction, when the reaction has proceeded to only 3% completion (1 turnover). Also, **2** was observed in the catalyst mixture during the reaction of phenylacetylene and *n*-propylamine (Table 1, entry 20); this reaction is not catalytic because **2** is not protonated by the weakly acidic *n*-propylammonium ion. To determine if complex **2** is involved in the catalytic cycle, it was used as the catalyst in the presence of 1 equiv of $\text{HBF}_4\cdot\text{OEt}_2$; these conditions resulted in the same yield of **A** (Table 1, entry 3).

In the catalytic reactions, the *p*-toluidinium ion ($\text{p}K_{\text{a}}(\text{H}_2\text{O}) = 5.1$) or the protonated iminium form of the product **A** ($\text{p}K_{\text{a}}(\text{H}_2\text{O}, \text{calculated}) \approx 4.9$)¹¹ serves as the acid for the protonation of **2** to give complexes **3a,b** (step C). This protonation of **2** occurs at either the internal or terminal carbon of the phenylacetylene ligand and can be observed after 1 h as a mixture of **2**, **3a,b**, **8**, and **A** in the ^1H NMR spectrum of a CD_2Cl_2 solution of **2** to which 1 equiv of $(4\text{-MeC}_6\text{H}_4)\text{NH}_3^+\text{BF}_4^-$ is added. The protonation reaction is greatly simplified by the use

(9) Ovchinnikov, M. V.; Guzei, I. A.; Angelici, R. J. *Organometallics* **2001**, *20*, 691.

(10) Ovchinnikov, M. V.; Klein, D. P.; Guzei, I. A.; Choi, M.-G.; Angelici, R. J. *Organometallics* **2002**, *21*, 617.

(11) Calculated using Advanced Chemistry Development (ACD) Software Solaris V4.67, 2004, located within Scifinder Scholar 2001.

of $\text{HBF}_4 \cdot \text{OEt}_2$ as the acid and cleanly gives the three isomers **3a**, **b**, and **7** (Scheme 1, step C) in the ratio 2:1:0.01 (**3a**:**3b**:**7**). The IR spectrum of the mixture in $\text{CH}_2\text{-Cl}_2$ exhibits bands at 2071 (s), 2048 (w), 2018 (vs), and 1994 (s) cm^{-1} , which indicates that there are no bridging CO groups in either of the major isomers. Although the isomers could not be separated, the mixture gave a correct elemental analysis and the complexes were characterized by their NMR spectra as described below. The protonation of **2** (step C) is apparently reversible, as the **3a/3b/7** mixture reacts with a 30-fold excess of Et_3N completely within 5 min at room temperature to give a 20% yield of **2**, but the other 80% of the Ru-containing products could not be identified and presumably resulted from other reactions of **3a/3b/7** with Et_3N .

The ^1H NMR spectrum of the major isomer, **3a**, exhibits four doublets and two triplets for the Cp proton resonances, indicating a completely unsymmetrical environment for the bridging $(\eta^5\text{-C}_5\text{H}_3)_2(\text{SiMe}_2)_2$ ligand. The low symmetry is also reflected in the four signals for the methyl groups bonded to silicon at -0.79 , 0.49 , 0.72 , 0.74 ppm; the peaks at 0.49 and -0.79 ppm are broad and shifted upfield due to shielding of the methyl groups by the phenyl group of the bridging vinyl moiety. The geminal protons exhibit ^1H NMR resonances at 4.51 and 3.37 ppm with a coupling constant of 2 Hz, which is typical for geminal protons in bridging vinyl ligands.⁸ The upfield position (3.37 ppm) of one of the geminal protons is consistent with shielding by the phenyl group. The geminal resonance at 3.37 ppm, along with those of the Si–Me groups at 0.49 and -0.79 ppm, is broad in the room-temperature spectrum of **3a**, presumably because of restricted rotation of the phenyl group; such broad signals have been observed in the methyl groups of the $(\eta^5\text{-C}_5\text{H}_3)_2(\text{SiMe}_2)_2$ ligand in diruthenium complexes containing the diphenylacetylene ligand.¹⁰ Cooling a CD_2Cl_2 solution containing **3a** to -25 °C gives an ^1H NMR spectrum with a sharp resonance at 3.32 ppm for the geminal proton and four sharp $\text{Si}(\text{CH}_3)_2$ resonances at -0.88 , 0.43 , 0.67 , and 0.69 ; these sharp resonances are consistent with a slow rotation of the phenyl group at the lower temperature. In the low-temperature ^1H NMR spectrum, the ratio of the two major isomers changes to approximately 4:1 (**3a**:**3b**), with the amount of **7** staying the same; this change in isomer ratio with temperature also indicates that the interconversion of isomers **3a**, **b** is rapid.

The room-temperature ^1H NMR spectrum of **3b** shows that it has a structure similar to that of **3a**. In contrast to the bridging vinyl group in **3a**, it is the phenyl group in **3b** that is coordinated to the ruthenium to give a bridging η^3 -benzyl derivative. Freely rotating phenyl groups exhibit one doublet and three triplets due to the plane of symmetry. However, in **3b** there is no plane of symmetry, as indicated by the four resonances for the benzyl group at 6.81 (d), 6.94 (d), 7.65 (m), and 7.69 (m); a similar pattern was observed by King for the η^3 -benzyl ligand in $\text{CpMo}(\text{CO})_2(\eta^3\text{-CH}_2\text{C}_6\text{H}_5)$.¹² Complex **3b** exhibits four resonances for the $\text{Si}(\text{CH}_3)_2$ groups at 0.84 , 0.58 , 0.55 , and 0.52 ppm and six resonances for the Cp protons at 5.05 , 5.42 , 5.63 , 5.94 , 6.18 , and 6.50 ppm, due to the low symmetry of the complex. Compared to

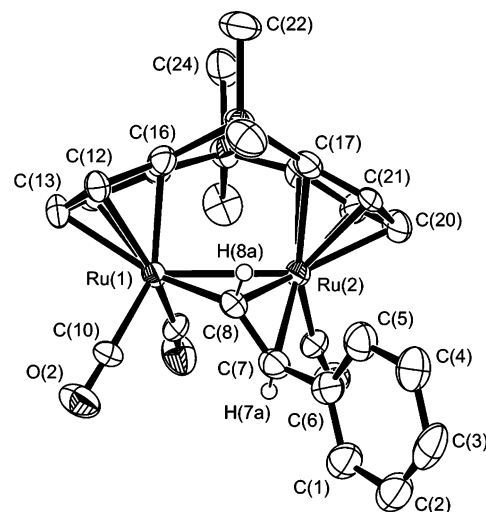


Figure 2. Thermal ellipsoid drawing of the cation in $[(\eta^5\text{-C}_5\text{H}_3)_2(\text{SiMe}_2)_2\text{Ru}(\text{CO})_3\{\text{trans-}\mu_2\text{-}\eta^1\text{-}\eta^2\text{-C}(\text{H})=\text{C}(\text{H})\text{Ph}\}][\text{BF}_4]$ (**7**) with 50% ellipsoid probability and labeling scheme. Hydrogen atoms are omitted for clarity. Selected bond distances (Å) and angles (deg): Ru(1)–Ru(2), 2.878(3); Ru(1)–C(8), 2.105(8); Ru(2)–C(8), 2.118; Ru(2)–C(7), 2.385; C(7)–C(8), 1.389(14); C(6)–C(7), 1.493(14); Ru(1)–Cp(centroid), 1.925; Ru(2)–Cp(centroid), 1.859; $\angle\text{C}(8)\text{–Ru}(1)\text{–Ru}(2)$, 47.2(2); $\angle\text{C}(6)\text{–C}(7)\text{–C}(8)$, 125.6(9); $\angle\text{Ru}(1)\text{–C}(8)\text{–C}(7)$, 129.9(8); $\angle\text{Ru}(2)\text{–C}(8)\text{–C}(7)$, 82.91; $\angle\text{Ru}(1)\text{–C}(8)\text{–Ru}(2)$, 85.95; $\angle\text{Ru}(1)\text{–C}(8)\text{–C}(7)\text{–C}(6)$, 8.9; $\angle\text{Cp(centroid)\text{–Ru}(1)\text{–Ru}(2)\text{–Cp(centroid)}$, 3.9; $\angle\text{Cp}\text{–Cp}$ fold angle, 125.1.

those (4.51 and 3.37 ppm) for **3a**, resonances for the geminal protons (3.80 and 4.17 ppm) of the vinyl ligand in **3b** are shifted much closer to each other. Although these protons are coupled to each other in the COSY NMR spectrum, the coupling constant was too small to measure, similar to what is observed in the σ -bonded vinyl ligand of $[\text{Ru}_2\{\eta^1\text{-C}(\text{Ph})=\text{CH}_2\}(\mu\text{-CO})_2(\text{CO})_2(\mu\text{-dppm})_2]^+$.^{13a}

The final isomer obtained from the protonation of **2** is **7**; in this isomer, the proton adds to the carbon in **2** that bears the phenyl group, and the two vinyl protons are trans to each other. These vinyl protons exhibit ^1H NMR resonances at 4.84 and 9.91 ppm that have a coupling constant of 11 Hz, as expected for bridging vinyl protons with a trans geometry.⁸ The ^1H NMR spectrum also exhibits four resonances for the $\text{Si}(\text{CH}_3)_2$ methyl groups at 0.63 , 0.69 , 0.70 , and 0.94 ppm and four resonances for the cyclopentadienyl protons at 5.09 , 5.70 , 6.19 , and 6.71 ppm (the peaks at 5.09 and 5.70 integrating for two protons each). Isomer **7** is more stable thermodynamically than **3a**, **b**, as heating (50 °C) of a dichloroethane solution of the **3a/3b/7** mixture for 18 h resulted in quantitative formation of isomer **7** (Scheme 1, step F). The molecular structure (Figure 2) of **7** has been determined by X-ray diffraction and confirms the trans geometry of the bridging vinyl ligand. Complex **7** contains a Ru–Ru bond (2.878(3) Å) that is 0.11 Å longer than that in parent complex **2** and 0.03 Å longer than that in the related ruthenium phosphine complex $[\text{Ru}_2(\text{CO})_4(\text{trans-}\mu_2\text{-}\eta^1\text{-}\eta^2\text{-CH}=\text{CHPh})(\mu\text{-dppm})_2]^+$.^{13b} The σ -Ru(1)–C(8) bond of the vinyl ligand is $2.105(8)$ Å, and the olefinic portion of the vinyl ligand is unsymmetrically bonded in an η^2 fashion to Ru(2), with the bridging C(8) atom being 0.27 Å closer than

(12) King, R. B.; Fronzaglia, A. *J. Am. Chem. Soc.* **1966**, *88*, 709.

the terminal C(7) atom (2.385 Å) to Ru(2). The unsymmetrical nature of this bond may be partially rationalized by steric repulsions between the Cp fragment on Ru(2) and the phenyl group, as indicated by a 2.457 Å distance between hydrogen atoms on C(5) of the cyclopentadienyl group and C(21) of the phenyl group. The C(8)–C(7) bond distance of the vinyl moiety is 1.389 Å, 0.07 Å longer than that in the phenylacetylene ligand in **2** but only slightly longer than a normal C=C double bond (1.34 Å). The double-bond character of the C(8)–C(7) bond is also supported by the 125.6(9) and 129.9(8)° angles for C(6)–C(7)–C(8) and Ru(1)–C(8)–C(7), respectively.

Attempts to use **7** as a catalyst precursor resulted in no catalytic activity, and although **7** is not directly involved in the catalytic reactions, its isomers **3a,b** are proposed to react (step *D*) by undergoing amine attack on the η^2 -coordinated vinyl group at the carbon bearing the phenyl group. This proposed site of attack is based on the structure of the imine product **A**, in which the N and Ph groups are bonded to the same carbon. As seen in other examples of amine attack on olefins coordinated to positive metal centers,¹⁴ the amine attack on the vinyl group in **3a** is presumably promoted by its η^2 coordination to a positive Ru center, but benzyl isomer **3b** is not similarly activated. Knox and co-workers⁸ previously reported the reaction of BH_4^- with $\text{Cp}_2\text{Ru}_2(\text{CO})_2(\mu\text{-CO})(\mu_2\text{-}\eta^1\text{-}\eta^2\text{-CH=CH}_2)^+$ to give products resulting from H^- attack on both the α - and β -carbons of the bridging vinyl ligand. The α -attack is analogous to that proposed in step *D*. In an attempt to characterize products of the nucleophilic reactions (step *D*), we added a 30-fold excess of *p*-toluidine at room temperature to a CD_2Cl_2 solution of the mixture of **3a,b**. Within 5 min of the amine addition, the ^1H NMR spectrum indicates the formation of **4** (Scheme 1, step *D*). The ^1H NMR spectrum of **4** exhibits resonances at 0.21 and 0.16 ppm for the methyl groups on $(\eta^5\text{-C}_5\text{H}_3)_2(\text{SiMe}_2)_2$ and resonances for the Cp fragments at 4.93 (d), 5.21 (d), 5.49 (t), and 6.01 (t) ppm. These resonances are similar to those of $\{(\eta^5\text{-C}_5\text{H}_3)_2(\text{SiMe}_2)_2\}\text{Ru}_2(\text{CO})_3(\text{C}_2\text{H}_4)$,⁴ whose resonances for the $\{(\eta^5\text{-C}_5\text{H}_3)_2(\text{SiMe}_2)_2\}$ ligand occur at 0.35, 0.44 (SiCH₃) and 4.88, 5.48, 5.79 (Cp *H*). Resonances for the two geminal protons of the coordinated enaminium ion are observed at 5.24 (d) and 5.70 (d) ppm with a coupling constant of 1.6 Hz, which is consistent with geminal protons in coordinated vinylic olefins.¹⁵ The geometry of these protons is also supported by the ^1H – ^{13}C -coupled NMR spectrum, which indicates that these protons reside on the same carbon, with a ^{13}C chemical shift of 127.2 ppm. Aromatic resonances for the *p*-toluidine group are observed as broad doublets at 4.86 and 5.76 ppm (*p*-MeC₆H₄), shifted upfield due to shielding by the adjacent phenyl ring. The methyl group of the *p*-toluidine fragment is observed at 2.28 ppm, and the protons of the phenyl ring are observed at 7.08 (m, 4 H) and 7.24 (t, 1 H) ppm. Complex **4** is also observed in the IR spectrum of a solution formed by the addition of a 30-fold excess of *p*-toluidine to a CH_2Cl_2 solution of

3a/3b at room temperature. The $\nu(\text{CO})$ bands at 2025 (vs) and 1965 (vs) cm^{-1} are at somewhat higher wavenumbers than those of the analogous ethylene complex, $\{(\eta^5\text{-C}_5\text{H}_3)_2(\text{SiMe}_2)_2\}\text{Ru}_2(\text{CO})_3(\text{C}_2\text{H}_4)$ (2000 (vs), 1950 (vs), 1923 (w) cm^{-1}),⁴ with the minor absorbance in **4** (corresponding to 1923 cm^{-1}) presumably being obscured by the broad peak at 1965 cm^{-1} . The higher wavenumbers of these bands in **4** are due to the electron-withdrawing nature of the phenyl ring and the ammonium group on the coordinated olefin. Attempts to isolate **4** were unsuccessful.

Also present after 5 min in the reaction of *p*-toluidine with **3a,b** in CD_2Cl_2 is approximately 6% of the protonated amine complex **8**, as indicated by resonances at 0.33, 0.43, 0.45, and 0.52 ppm for the methyl groups located on the SiMe₂ groups in the ^1H NMR spectrum; complete conversion of **4** to **8** was achieved after approximately 18 h at room temperature. Complex **8** was isolated from the reaction of a 30-fold excess of *p*-toluidine with isomers **3a,b** in a CH_2Cl_2 solution after 18 h at room temperature (Scheme 1, steps *D*, *E*, *H*). The ^1H NMR spectrum of **8** exhibits one resonance for the bridging hydride ligand at –18.98 ppm, four resonances for the methyl groups of the bridging SiMe₂ groups, one resonance for the *p*-methyl group of the coordinated amine at 2.25 ppm, one resonance for the –NH₂ group at 5.42 ppm, five resonances at 5.12, 5.61, 5.64, 5.78, and 5.90 ppm for the Cp fragments, and resonances at 6.85 and 7.03 ppm for the aryl protons of the coordinated amine. The IR spectrum of **8** in CH_2Cl_2 exhibits only terminal $\nu(\text{CO})$ bands (2052 (vs), 2004 (vs), and 1960 (w) cm^{-1}) that are shifted to wavenumbers slightly higher than those (2050 (vs), 2002 (vs), 1954 (w) cm^{-1}) of the previously characterized protonated pyrrolidine complex $\{(\eta^5\text{-C}_5\text{H}_3)_2(\text{SiMe}_2)_2\}\text{Ru}_2(\text{CO})_3(\text{NH}(\text{CH}_2\text{CH}_2)_2)\text{H}^+\text{BF}_4^-$,⁹ as expected for the less electron-donating *p*-toluidine ligand.

When the reaction of **3a,b** with *p*-toluidine (30-fold excess) in CD_2Cl_2 at room temperature was conducted in the presence of a 30-fold excess of phenylacetylene, still the only product was **8**. Thus, intermediate **5** does not react with phenylacetylene under these conditions to give **2**, which indicates that **5** is converted to **8** faster than it is converted to **2**. The slow conversion of **5** to **2** is consistent with the observation that, in the synthesis of **2**, the reaction of $\{(\eta^5\text{-C}_5\text{H}_3)_2(\text{SiMe}_2)_2\}\text{Ru}_2(\text{CO})_3(\text{NHMe}_2)$ with phenylacetylene requires heating to 50 °C (Scheme 2). The fact that the **3a,b**-catalyzed reaction of phenylacetylene with *p*-toluidine requires 40 °C indicates that the conversion of **5** to **2** does occur at this temperature (entry 2, Table 1). While **8** probably forms during the catalytic reaction, it is in equilibrium with **5** (step *H*), which is supported by the observation that **8** catalyzes the reaction of phenylacetylene with *p*-toluidine (30-fold excess) in CD_2Cl_2 at 40 °C to give the expected imine product (entry 7, Table 1). Attempts to prepare **5** by reaction of **1** with *p*-toluidine according to eq 2 and by the deprotonation of **8** with Et₃N were unsuccessful.

While the results discussed above provide good evidence for the proposed catalytic cycle (Scheme 1), it is also necessary to account for the short lifetime (up to 6 turnovers) of the catalyst. Since the vinylidene complex **6** is the only form of ruthenium that exists in the

(13) (a) Gao, Y.; Jennings, M. C.; Puddephatt, R. J. *Dalton* **2003**, 261. (b) Gao, Y.; Jennings, M. C.; Puddephatt, R. J. *Can. J. Chem.* **2001**, *79*, 915.

(14) Bush, R. C.; Angelici, R. J. *J. Am. Chem. Soc.* **1986**, *108*, 2735.

(15) Chang, T. C. T.; Coolbaugh, T. S.; Foxman, B. M.; Rosenblum, M.; Simms, N.; Stockman, C. *Organometallics* **1987**, *6*, 2394.

reaction solution when the catalyst becomes inactive, it is the formation of **6** that terminates the reaction. The two most likely routes to the formation of **6** are direct isomerization of **2** to **6** and the deprotonation of the α -carbon in **7**. Heating a CD_2Cl_2 solution of **2** at 40 °C (the temperature of the catalytic studies) for 18 h resulted in the formation of **6** in approximately 40% yield (Scheme 1, step G). Thus, it is possible that the isomerization of **2**, the predominant species in the catalytic reactions, is responsible for the formation of **6**. To determine if **6** is formed by the deprotonation of **7**, a 30-fold excess of *p*-toluidine was reacted with **7** at room temperature, but even after 18 h 50% of **7** remained, and there was no evidence for **6**; however, the ^1H NMR spectrum indicated the formation of other unidentifiable Ru-containing products. Thus, it is the isomerization of **2** to **6** (step G) that appears to be the major reason for the inactivation of the catalyst.

Conclusion

These investigations show that the dinuclear complexes **1**, **3a,b**, and **8** containing the doubly bridged cyclopentadienyl ligand $(\eta^5\text{-C}_5\text{H}_3)_2(\text{SiMe}_2)_2$ catalyze the hydroamination of arylalkynes by reaction with arylamines. The catalytic activity of these complexes is a result of the unique bridging nature of the cyclopentadienyl ligand, as the nonbridged complex $\{(\eta^5\text{-C}_5\text{H}_5)_2\text{Ru}_2(\text{CO})_2(\mu\text{-CO})\{\mu_2\text{-}\eta^1\text{:}\eta^2\text{-C(Ph)=CH}_2\}\}^+\text{BF}_4^-$, an analogue of **3a**, does not catalyze the reaction. The proposed mechanism (Scheme 1) is based on the isolation and structural characterization (X-ray and/or NMR) of the following intermediates (or close analogues): **1**, **2**, **3a,b**, **4**, **6**, **7**, and **8**. The role of **2** as an intermediate in the catalytic cycle is supported by its presence during the reaction and its ability to catalyze the reaction in the presence of $\text{HBF}_4\cdot\text{OEt}_2$. When intermediates **3a,b** are reacted with *p*-toluidine at room temperature, they give the expected imine **A**, as well as complexes **4** and **8**. Thus, key identified intermediates react as expected, according to Scheme 1, under the conditions of the catalytic reactions. The inactivation of the catalyst occurs primarily by the isomerization of **2** to its vinylidene isomer **6**, which is not catalytic. The present catalytic system, although not as useful for the synthesis of imines as other methods, does reveal details of the mechanism by which diruthenium complexes catalyze the hydroamination of alkynes. The mechanism is fundamentally different from those proposed for hydroamination reactions that are catalyzed by mononuclear transition-metal complexes.

Experimental Section

General Considerations. All reactions were carried out under an inert atmosphere of dry argon using standard Schlenk techniques. Diethyl ether, methylene chloride, and hexanes were purified on alumina using a Solv-Tek solvent purification system, similar to that reported by Grubbs.¹⁶ Methylene chloride-*d*₂ was stirred overnight with calcium hydride and then refluxed for 4 h and distilled over calcium hydride. Acetone-*d*₆ was distilled from CaSO_4 , and DMSO-*d*₆ was vacuum-distilled from NaOH. Dichloroethane was distilled

from P_2O_5 , *N*-methylaniline and *n*-propylamine were stirred with KOH overnight and fractionally distilled, and *p*-toluidine was recrystallized first from ethanol and then from boiling hexanes. Complexes $\{(\eta^5\text{-C}_5\text{H}_3)_2(\text{SiMe}_2)_2\text{Ru}_2(\text{CO})_3(\text{C}_2\text{H}_4)\text{H}^+\text{BF}_4^-$ (**1**),⁴ $\{(\eta^5\text{-C}_5\text{H}_3)_2(\text{SiMe}_2)_2\text{Ru}_2(\text{CO})_4\text{H}^+\text{BF}_4^-$,¹⁷ and $(\eta^5\text{-C}_5\text{H}_5)_2\text{Ru}_2(\text{CO})_2(\mu\text{-CO})\{\mu_2\text{-}\eta^1\text{:}\eta^2\text{-C(Ph)=CH}_2\}^+\text{BF}_4^-$ ⁸ were prepared by reported methods. All other compounds were used as received from Aldrich. Solution infrared spectra were recorded on a Nicolet-560 spectrometer using NaCl cells with a 0.1 mm path length. ^1H and ^{13}C NMR spectra were recorded on Bruker DRX-400, Varian VXR-300, and Bruker AC-200 spectrometers using deuterated solvent signals as internal references. Elemental analyses were performed on a Perkin-Elmer 2400 Series II CHNS/O analyzer.

Synthesis of $\{(\eta^5\text{-C}_5\text{H}_3)_2(\text{SiMe}_2)_2\text{Ru}_2(\text{CO})_2(\mu\text{-CO})\{\mu_2\text{-}\eta^1\text{:}\eta^2\text{-C(Ph)=C(H)}\}$ (2**).** Anhydrous gaseous NMe_2H (23 mL, 0.94 mmol) was bubbled by syringe into a CH_2Cl_2 (20 mL) solution of $\{(\eta^5\text{-C}_5\text{H}_3)_2(\text{SiMe}_2)_2\text{Ru}_2(\text{CO})_4\text{H}^+\text{BF}_4^-$ (200 mg, 0.310 mmol). After 1 h, solvent was removed under vacuum, the residue was redissolved in 10 mL of hexanes, and phenylacetylene (0.34 mL, 3.1 mmol) was added. The solution was then heated to 50 °C for 30 min while the reaction mixture turned from red to orange. Upon cooling, reduction of the solvent volume to about 3 mL caused the precipitation of **2**, which was separated by filtration. The product was then washed with 10 mL of hexanes, followed by three additional washes with cold hexanes (5 mL), each wash being removed by filtration. Drying under vacuum gave 110 mg of **2** (56% yield). Crystals suitable for X-ray diffraction were grown by layering a CH_2Cl_2 (3 mL) solution of **2** (50 mg) with hexanes (30 mL), and cooling to -30 °C. ^1H NMR (400 MHz, CD_2Cl_2): δ 0.27 (s, 3 H, Si(CH_3)), 0.37 (s, 3 H, Si(CH_3)), 0.45 (s, 3 H, Si(CH_3)), 0.52 (s, 3 H, Si(CH_3)), 5.21 (m, 1 H, Cp H), 5.26 (m, 1 H, Cp H), 5.66 (m, 1 H, Cp H), 5.69 (m, 1 H, Cp H), 6.41 (t, $J = 2$ Hz, 1 H, Cp H), 6.43 (t, $J = 2.4$ Hz, 1 H, Cp H), 7.10 (t, $J = 7.2$ Hz, 1 H, Ph H), 7.26 (t, $J = 7.2$ Hz, 2 H, Ph H), 7.42 (m, 2 H, Ph H), 8.46 (s, 1 H, PhC \equiv CH). ^{13}C NMR (50 MHz, CD_2Cl_2): δ -3.08, -2.24, 2.11, 6.56 (Si(CH_3)), 91.69, 92.50, 93.71, 96.11, 97.22, 97.52, 99.31, 100.82 (Cp C), 104.19 (br, PhC \equiv CH), 114.13, 114.33 (Cp C), 129.70, 128.15, 129.09, 142.83 (Ph C), 204.05, 204.76 (CO), 236.97 ($\mu\text{-CO}$). IR (CH_2Cl_2): $\nu(\text{CO})$ (cm^{-1}) 1996 (vs), 1965 (s), 1772 (w). Anal. Calcd for $\text{C}_{25}\text{H}_{24}\text{O}_3\text{Ru}_2\text{Si}_2$: C, 47.60; H, 3.84. Found: C, 47.29; H, 4.22.

Synthesis of $\{(\eta^5\text{-C}_5\text{H}_3)_2(\text{SiMe}_2)_2\text{Ru}_2(\text{CO})_3(\mu_2\text{-PhC}_2\text{-H}_2)^+\text{BF}_4^-$ (3a,b**).** Reaction of **2** (50 mg, 0.079 mmol) in CH_2Cl_2 (10 mL) with $\text{HBF}_4\cdot\text{OEt}_2$ (15 μL , 0.12 mmol) resulted in a darkening of the solution. After 1 h, solvent was reduced under vacuum to approximately 3 mL, and Et_2O (30 mL) was added to yield an orange oil. Careful decanting of the solvent gave an oily residue, which was dissolved in CH_2Cl_2 (5 mL); addition of hexanes (40 mL) to this solution precipitated the mixture of **3a,b**. Filtration, followed by drying under vacuum, gave 40.8 mg (72% yield) of a mixture of two isomers, **3a,b**. Major isomer, **3a**: ^1H NMR (400 MHz, CD_2Cl_2 , -25 °C) δ -0.88 (s, 3 H, Si(CH_3)), 0.43 (s, 3 H, Si(CH_3)), 0.67 (s, 3 H, Si(CH_3)), 0.69 (s, 3 H, Si(CH_3)), 3.32 (d, $J = 2$ Hz, 1 H, C(Ph)=C(H)₂), 4.45 (d, $J = 2$ Hz, 1 H, C(Ph)=C(H)₂), 5.32 (m, 1 H, Cp H), 5.58 (m, 1 H, Cp H), 5.62 (m, 1 H, Cp H), 5.79 (m, 1 H, Cp H), 6.03 (m, 1 H, Cp H), 6.89 (t, $J = 2$ Hz, 1 H, Cp H), 7.33 (m, 5 H, C(Ph)=C(H)₂); ^{13}C NMR (100 MHz, CD_2Cl_2 , -25 °C): δ -7.53, 0.24, 3.90, 5.79 (Si(CH_3)), 69.65 (C(Ph)=C(H)₂), 81.86, 93.70, 94.33, 95.62, 98.54, 109.12 (Cp C), 128.57, 128.89, 152.38, 172.02 (Ph C), 193.93, 195.60, 206.49 (CO). Minor isomer, **3b**: ^1H NMR (400 MHz, CD_2Cl_2 , -25 °C) δ 0.47 (s, 3 H, Si(CH_3)), 0.50 (s, 3 H, Si(CH_3)), 0.53 (s, 3 H, Si(CH_3)), 0.80 (s, 3 H, Si(CH_3)), 3.73 (s, 1 H, C(Ph)=C(H)₂), 4.14 (s, 1 H, C(Ph)=C(H)₂), 5.03 (m, 1 H, Cp H), 5.40 (t, $J = 2.4$ Hz, 1 H, Cp H), 5.60 (m, 1 H, Cp H), 5.91 (d, $J = 2$ Hz, 1 H, Cp H), 6.16 (m, 1 H, Cp H), 6.51 (m, 1

(16) Pangborn, A. B.; Giardello, M. A.; Grubbs, R. H.; Rosen, R. K.; Timmers, F. J. *Organometallics* **1996**, *15*, 1518.

(17) Ovchinnikov, M. V.; Angelici, R. J. *J. Am. Chem. Soc.* **2000**, *122*, 6130.

H, Cp H), 6.71 (d, $J = 7.2$ Hz, 1 H, o-H of Ph), 6.93 (d, $J = 7.8$ Hz, 1 H, o-H of Ph), 7.57 (m, 1 H, p-H of Ph), 7.66 (m, 2 H, m-H of Ph); ^{13}C NMR (100 MHz, CD_2Cl_2 , -25°C): δ -4.42, -2.38, 0.88, 1.50 (Si(CH₃)), 65.89 (C(Ph)=C(H)₂), 78.81, 87.22, 90.84, 99.11, 100.18, 101.12 (Cp C), 78.44, 125.83, 132.26, 134.68, 136.45 (Ph C), 196.45, 197.97, 201.37 (CO). Resonances in the ^{13}C NMR spectrum of **3a,b** are assigned on the basis of a heteronuclear (^1H - ^{13}C) coupling experiment. The ^{13}C NMR spectrum of the mixture also contained the correct number of resonances for the quaternary carbon atoms of both **3a** and **3b**; however, these peaks could not be assigned. IR (**3a,b**, $\text{CH}_2\text{-Cl}_2$): $\nu(\text{CO})$ (cm^{-1}) 2071 (s), 2048 (w), 2018 (vs), 1994 (s). Anal. Calcd for $\text{C}_{25}\text{H}_{25}\text{O}_3\text{Ru}_2\text{Si}_2\text{BF}_4$: C, 41.79; H, 3.51. Found: C, 41.80; H, 3.90.

Synthesis of $\{(\eta^5\text{-C}_5\text{H}_5)_2(\text{SiMe}_2)_2\text{Ru}_2(\text{CO})_3\{\text{trans-}\mu_2\text{-}\eta^1\text{-}\eta^2\text{-C(H)=C(H)Ph}\}^+\text{BF}_4^-\}$ (7**).** A dichloroethane (10 mL) solution of **2** (50 mg, 0.079 mmol) was treated with $\text{HBF}_4\cdot\text{OEt}_2$ (15 μL , 0.12 mmol) and heated to 50°C for 12 h. The solvent was reduced under vacuum to approximately 3 mL, and hexanes (50 mL) was added to precipitate **7**. Filtration of the solution, followed by solvent removal under vacuum, gave **7** (43 mg, 76%). Crystals suitable for X-ray diffraction were grown by layering a CH_2Cl_2 (2 mL) solution of **7** (25 mg) with Et_2O (25 mL) and cooling to -30°C . ^1H NMR (400 MHz, $\text{CD}_2\text{-Cl}_2$): δ 0.63 (s, 3 H, Si(CH₃)), 0.69 (s, 3 H, Si(CH₃)), 0.70 (s, 3 H, Si(CH₃)), 0.94 (s, 3 H, Si(CH₃)), 4.84 (d, $J = 10.8$ Hz, 1 H, C(H)=CPh(H)), 5.09 (m, 2 H, Cp H), 5.70 (m, 2 H, Cp H), 6.19 (m, 1 H, Cp H), 6.71 (m, 1 H, Cp H), 7.29 (m, 5 H, C(H)=C(Ph H)H), 9.91 (d, $J = 10.8$ Hz, 1 H, C(H)=CPh(H)). ^{13}C NMR (100 MHz, CD_2Cl_2): δ -3.72, -1.40, 2.31, 5.86 (Si(CH₃)), 82.35, 93.10, 93.49, 93.94, 96.66, 97.14, 98.89, 102.00, 105.64, 118.21 (Cp C), 83.94, 137.70 (μ -vinyl); 126.20, 128.75, 129.62, 141.63, (Ph C), 193.13, 196.51 (CO). IR (CH_2Cl_2): $\nu(\text{CO})$ (cm^{-1}) 2072 (s), 2017 (vs), 1986 (w). Anal. Calcd for $\text{C}_{25}\text{H}_{25}\text{O}_3\text{Ru}_2\text{Si}_2\text{BF}_4$: C, 41.79; H, 3.51. Found: C, 41.41; H, 3.78.

Synthesis of $\{(\eta^5\text{-C}_5\text{H}_5)_2(\text{SiMe}_2)_2\text{Ru}_2(\text{CO})_3[\text{NH}_2(p\text{-Me-C}_6\text{H}_4)]\text{H}^+\text{BF}_4^-\}$ (8**).** To a CH_2Cl_2 (10 mL) solution of the mixture of isomers **3a,b** (25 mg, 0.035 mmol) was added *p*-toluidine (112 mg, 1.04 mmol), and the solution was stirred for 18 h. The volume of the solution was then reduced to 2 mL under vacuum. Addition of 30 mL of Et_2O , followed by filtration, gave **8** as a maroon powder (16.5 mg, 65% yield). ^1H NMR (400 MHz, CD_2Cl_2): δ -18.98 (s, 1H, Ru-H-Ru), 0.33 (s, 3 H, Si(CH₃)), 0.43 (s, 3 H, Si(CH₃)), 0.45 (s, 3 H, Si(CH₃)), 0.52 (s, 3 H, Si(CH₃)), 2.25 (s, 3 H, *p*-CH₃C₆H₄NH₂), 5.12 (m, 1 H, Cp H), 5.42 (m, 2 H, *p*-CH₃C₆H₄NH₂), 5.61 (t, $J = 2$ Hz, 1 H, Cp H), 5.64 (m, 1 H, Cp H), 5.78 (m, 2 H, Cp H), 5.90 (m, 1 H, Cp H), 6.85 (d, $J = 8$ Hz, 2 H, *p*-CH₃C₆H₄NH₂), 7.03 (d, $J = 8$ Hz, 2 H, *p*-CH₃C₆H₄NH₂). ^{13}C NMR (100 MHz, CD_2Cl_2): δ -3.00, 2.17, 3.67 (Si(CH₃)), 20.77 (NH₂(*p*-MeC₆H₄)), 70.87, 81.50, 87.94, 89.77, 93.88, 95.22, 99.08, 102.89, 103.83, 104.59 (Cp C), 120.03, 130.34, 135.17, 144.89 (Ph C), 196.00, 197.50, 203.40 (CO). IR (CH_2Cl_2): $\nu(\text{CO})$ (cm^{-1}) 2052 (vs), 2004 (vs), 1960 (w). Anal. Calcd for $\text{C}_{21}\text{H}_{28}\text{BF}_4\text{NO}_3\text{Ru}_2\text{Si}_2$: C, 39.84; H, 3.90; N, 1.94. Found: C, 39.80; H, 3.91; N, 1.80.

General Procedure for the Catalytic Hydroamination Reaction. In a typical catalytic run, the catalyst precursor (approximately 5–7 mg) was loaded into an NMR tube, and the tube was run through three vacuum/Ar flush cycles. Under Ar, the alkyne, the amine, 5 μL of *N,N*-dimethylacetamide (DMAC, internal standard), and 0.6 mL of dry CD_2Cl_2 were then added. The solution was then frozen with liquid nitrogen and subjected to three freeze/pump/thaw cycles; the tube was flame-sealed under dynamic vacuum on the fourth cycle. The NMR tube was then placed in a constant-temperature oil bath at $40.0 \pm 1.0^\circ\text{C}$, and the ^1H NMR spectrum was recorded after 18 h. The yield of the imine was determined by the ratio of the methyl peak of the *p*-MeC₆H₄ or the -C(=NR)Me group of the imine to the reference -C(O)Me peak of DMAC. Results of these reactions are summarized in Table 1. Imines were identified by comparison of their ^1H NMR spectra in CD_2Cl_2

Table 2. Crystal Data and Structure Refinement Details for **2 and **7****

	2	7
empirical formula	$\text{C}_{25}\text{H}_{24}\text{O}_3\text{Ru}_2\text{Si}_2$	$\text{C}_{25}\text{H}_{25}\text{BF}_4\text{O}_3\text{Ru}_2\text{Si}_2$
formula wt	630.76	718.58
tempo, K	173(2)	193(2)
wavelength, Å	0.710 73	0.710 73
cryst syst	monoclinic	monoclinic
space group	$C2/c$	$P2_1$
unit cell dimens		
<i>a</i> , Å	35.495(7)	9.280(10)
<i>b</i> , Å	8.7563(16)	12.903(14)
<i>c</i> , Å	15.913(3)	12.147(13)
α , deg	90	90
β , deg	105.490(5)	108.389(17)
γ , deg	90	90
<i>V</i> , Å ³	4766.2(15)	1380(3)
<i>Z</i>	8	2
calcd density, Mg/m ³	1.758	1.729
abs coeff, mm ⁻¹	1.393	1.234
<i>F</i> (000)	2512	712
cryst size, mm ³	$0.47 \times 0.25 \times 0.12$	$0.30 \times 0.10 \times 0.10$
θ range for data	2.38–28.26	1.77–28.20
collec, deg		
index ranges	$-46 \leq h \leq 37,$ $-11 \leq k \leq 11,$ $-21 \leq l \leq 21$	$-12 \leq h \leq 12,$ $-15 \leq k \leq 16,$ $-15 \leq l \leq 15$
no. of rflns collected	18 794	10 309
no. of indep rflns	5522 ($R(\text{int}) =$ 0.0637)	5556 ($R(\text{int}) =$ 0.0748)
abs cor	empirical	semiempirical from equivalents
no. of data/restraints/ params	5522/0/293	5556/1/334
goodness of fit on F^2	1.048	1.119
final <i>R</i> indices	$R1 = 0.0287,$ $wR2 = 0.0745$	$R1 = 0.0489,$ $wR2 = 0.1210$
$(I > 2\sigma(I))$		
<i>R</i> indices (all data)	$R1 = 0.0332,$ $wR2 = 0.0765$	$R1 = 0.0764,$ $wR2 = 0.1585$
largest diff peak and hole, e/Å ³	0.983 and -0.687	1.779 and -1.042

to their literature-reported data (*n*-hexyl)MeC=N(*p*-MeC₆H₄),¹⁸ data from their independent syntheses (Ph)MeC=N(*p*-MeC₆H₄) and (Ph)MeC=N(Ph),¹⁹ or data from a newly prepared sample by an extension of a literature method (below) (*p*-FC₆H₄)MeC=N(*p*-MeC₆H₄).¹⁹

Synthesis of (*p*-FC₆H₄)MeC=N(*p*-MeC₆H₄). In a reaction analogous to that used in the synthesis of (*p*-MeOC₆H₄)MeC=N(*p*-MeC₆H₄),¹⁹ mercury(II) acetate (2.56 g, 8.03 mmol) was added to a THF (16 mL) solution of *p*-FC₆H₄C≡CH (0.92 mL, 8.03 mmol) and *p*-toluidine (0.857 g, 8.00 mmol). The reaction mixture was stirred for 1.75 h, after which 35 mL of 0.5 N aqueous NaOH was added. Immediately following the NaOH addition, sodium borohydride (0.605 g, 16.8 mmol) in 2 N NaOH (8 mL) was added, and the reaction mixture was stirred for an additional 3 h. The product was extracted with two portions of diethyl ether (15 mL), and the ether extract was dried with anhydrous sodium sulfate and filtered. The ether was removed under vacuum, and the residue was recrystallized from hexanes to give (*p*-FC₆H₄)MeC=N(*p*-MeC₆H₄) (0.42 g, 23% yield). Mp: 97–99 °C. ^1H NMR (400 MHz, CD_2Cl_2): δ 2.20 (s, 3 H, CH₃C=N), 2.34 (s, 3 H, *p*-MeC₆H₄N=C), 6.65 (m, 2 H), 7.13 (m, 4 H), 7.98 (m, 2 H). ^{13}C NMR (100 MHz, $\text{CD}_2\text{-Cl}_2$): δ 17.28 (CH₃C=N), 20.90 (*p*-MeC₆H₄), 115.31 (d, $J = 21.8$ Hz, *p*-FC₆H₄), 119.63 (*p*-MeC₆H₄), 129.54 (d, $J = 8.4$ Hz, *p*-FC₆H₄), 129.82 (*p*-MeC₆H₄), 133.04 (*p*-MeC₆H₄), 136.36 (d, $J = 2.7$ Hz, *p*-FC₆H₄), 149.37 (*p*-MeC₆H₄), 163.30 (d, $J = 247.9$ Hz, *p*-FC₆H₄), 164.21 (C=N). Anal. Calcd for $\text{C}_{15}\text{H}_{14}\text{FN}$: C, 79.27; H, 6.21; N, 6.16. Found: C, 79.04; H, 6.46; N, 6.14.

Molecular Structure Determinations of **2 and **7**.** The crystal evaluations and data collections were performed at 173

(18) Hartung, C. G.; Tillack, A.; Trauthwein, H.; Beller, M. *J. Org. Chem.* **2001**, *66*, 6339.

(19) Barluenga, J.; Aznar, F. *Synthesis* **1975**, 704.

K (**2**) or 193 K (**7**) on a Bruker CCD-1000 diffractometer with Mo K α ($\lambda = 0.71073 \text{ \AA}$) radiation and a detector-to-crystal distance of 5.03 cm. The data (Table 2) were collected using the full-sphere routine and were corrected for Lorentz and polarization effects. The absorption correction was based on fitting a function to the empirical transmission surface, as sampled by multiple equivalent measurements using SADABS software.^{20,21}

The structure solutions were accomplished by direct methods. All non-hydrogen atoms were refined by using a full-matrix anisotropic approximation. All hydrogen atoms were placed in the structure factor calculations at idealized positions

(20) Blessing, R. H. *Acta Crystallogr.* **1995**, *A51*, 33–38.

(21) All software and sources of the scattering factors are contained in the SHELXTL (version 5.1) program library (G. Sheldrick, Bruker Analytical X-ray Systems, Madison, WI).

and were allowed to ride on the neighboring atoms with relative isotropic displacement coefficients.

Acknowledgment. This work was supported by the National Science Foundation through Grant No. CHE-9816342.

Supporting Information Available: CIF files and tables giving crystallographic data for **2** and **7**, including atomic coordinates, bond lengths and angles, and anisotropic displacement parameters, low-temperature ($-25 \text{ }^\circ\text{C}$) ^1H , ^{13}C , COSY, and HETCOR NMR data for **3a,b**, ^1H , COSY, and HETCOR NMR data for **4**, and HETCOR NMR data for **7**. This material is available free of charge via the Internet at <http://pubs.acs.org>.

OM049377U